Solving coupled equations by iteration for heavy-ion multiple Coulomb-nuclear excitation

L. D. Tolsma
Department of Physics, Eindhoven University of Technology, Eindhoven, The Netherlands
(Received 1 July 1986)

To describe quantum mechanically multiple Coulomb-nuclear excitation in heavy-ion reactions, the set of coupled differential equations of the partial-wave radial solutions is rewritten in integral form. Decomposing these solutions into two basis functions, the corresponding amplitudes of these functions satisfy a set of coupled integral equations. Expressing the basis functions in terms of appropriately chosen piecewise analytic reference solutions, the integrals appearing in this set can be evaluated analytically. The coupled set of amplitude equations is solved iteratively. The efficiency of two iteration methods, the inward-outward and the sequential one, has been investigated for test cases dealing with multiple Coulomb and nuclear excitation of ^{238}U by 286 MeV ^{40}Ar and 718 MeV ^{84}Kr up to high spin states of the ground-state rotational band. Padé approximants to the S-matrix elements were also included in both of the iteration methods. It turns out that the inward-outward iteration method converges much faster than the sequential one. In many cases, the inward-outward method does not need Padé acceleration at all, while the sequential method does. It happens that convergent cases in the inward-outward method diverge in the sequential method aided by Padé approximants. Numerical studies of the excitation probabilities as a function of the scattering angle for the aforementioned heavy-ion reactions show that the probability functions of the members of the ground-state rotational band satisfy a general rule at near-grazing angles, previously formulated for the excitation probability as a function of the energy near the Coulomb barrier for backward scattering from a deformed rotor.

I. INTRODUCTION

The quantum-mechanical description of inelastic scattering of charged particles from nuclei requires the solution of the Schrödinger equation, which can be reformulated as a set of N coupled linear second-order differential equations of the partial-wave radial functions. Such a description becomes computationally intense when heavy ions are involved in the scattering process, mainly due to:

1. the rapidly oscillating behavior of the solution function within the classically allowed region of the integration range;
2. the long range of the Coulomb coupling—therefore, the integration of the set of coupled equations should be carried out over long ranges;
3. the large number of coupled equations or channels that, in general, should be considered;
4. the large number of partial waves that should be included when calculating the quantities observed.

In the usual approach, the set of coupled equations is solved as many times as the dimension of the set with linearly independent regular starting values at the origin for each of the solution vectors. The equations are integrated from the origin to a radius at which all nuclear and coupling interactions become insignificant. By constructing the physical solution as a linear combination of the solution vectors with the appropriate asymptotic behavior of an incoming partial wave in the entrance channel plus outgoing partial waves in all the relevant exit channels, the desired S-matrix elements can be found. This standard procedure is satisfactory for small systems of coupled equations, i.e., for light-ion reactions, but is particularly time consuming for the large systems associated with heavy-ion collisions. In addition, this procedure generates S-matrix elements which form a complete $N \times N$ matrix. However, in the nuclear physics context, often only a restricted number of entrance channels (only one for a zero-spin ground state) is important, which means that only a restricted number of columns of the scattering matrix are needed. In these cases, iteration methods can be applied for which the solutions are obtained directly without the need for solving the set of coupled equations N times.

The set of coupled equations can be integrated by means of the well-known multistep methods, such as the Numerov method. In applying these methods special attention has to be paid to the behavior of the solution. The heavier the charged particles in the scattering process and the higher the energy of their relative motion, the more rapidly the solution will oscillate in the classically allowed region and the smaller the step sizes in the multistep methods have to be chosen. Since these circumstances occur, in general, together with large systems of coupled equations and a long range of the Coulomb coupling, the multistep methods can become prohibitively time consuming.

In order to cope with the problems that occur in heavy-ion collisions, due to the standard procedure for solving the N coupled radial equations N times and due to the step-size dependency of the multistep methods, it is advantageous to formulate piecewise analytical solution methods together with iteration methods. In this way, an

efficient treatment of heavy-ion multiple Coulomb excitation was discussed in a previous paper.[1] It was shown that the partial-wave radial solution of the Schrödinger equation can be decomposed into regular and outgoing components, i.e., can be written as a linear combination of two basis functions which oscillate in the classically allowed region with relatively slowly varying amplitudes. These basis functions are the solutions of the decoupled radial equations. An appropriately chosen reference potential will allow them to be expressed in terms of piecewise analytic reference solutions. The efficiency of these methods depends upon the possibility of dividing the integration range into intervals which are sufficiently small to approximate the potential by some simpler varying reference potential, but which, on the other hand, contains a sufficiently large number of oscillations of the solution. It was also shown that, after rewriting the set of coupled differential equations into an integral form, the varying amplitudes satisfy a set of coupled integral equations. The integrals that arise in these equations can be evaluated analytically when Airy functions are used as piecewise analytic reference solutions corresponding to a linear reference potential.[2] The set of integral equations was solved by means of an iteration procedure. Two iteration schemes, an inward-outward[3,4] and a sequential or perturbative one,[5,6] were investigated. It appeared that only the inward-outward iteration scheme is of practical importance.

In an extended study about techniques for heavy-ion coupled channel calculations which include nuclear and Coulomb interactions, Rhoades-Brown *et al.* compared various iterative methods in order to solve the coupled radial equations in the interior region of configuration space.[7,8] The Born-Neumann series, the method of moments, Austern's modification of the Sasakawa method, and the sequential iteration were studied, but not in the inward-outward iteration. The conclusion was drawn that sequential iteration with Padé acceleration is the most rapidly convergent and efficient method. The integration of the set of coupled equations itself was carried out by means of a multistep method.

In this paper we report the continuation of our investigation into the numerical solution of the radial Schrödinger equation in order to describe heavy-ion multiple excitation including nuclear interactions. This was done within the framework of the iterative piecewise analytical solution method too. The approximation of the potential by a linear reference potential implies the generation of complex Airy functions[9,10] for the intervals of the integration region where the optical potential contributes significantly to the total interaction. However, since the numerical evaluation of complex Airy functions is rather computer time consuming, approximation of the potential by a constant reference potential has been investigated for this part of the integration range.[11] It appears that this approach is much more efficient, because the corresponding reference solutions are goniometric functions. In addition, Coulomb wave functions have been used as piecewise analytic reference solutions within the long range of the Coulomb coupling. The Coulomb integrals that arise in the coupled integral equations for the amplitudes can be efficiently evaluated using their recursion relations.[12] The efficiency of both iteration methods, the inward-outward and the sequential one, has been investigated for test cases dealing with multiple Coulomb and nuclear excitation of ^{238}U by 286 MeV ^{40}Ar and 718 MeV ^{84}Kr up to high spin states of the ground-state rotational band. Padé approximants to the S-matrix elements were also included in both of the iteration methods. It turns out that the inward-outward iteration method is still the most rapidly convergent one, and, even in many cases, it does not need Padé acceleration at all, while the sequential iteration method does. The first results of our investigation have been published already.[13,14]

The set of coupled second-order differential equations of the partial-wave radial functions can be rewritten equivalently into two sets of coupled first-order differential equations of the above-mentioned amplitudes. In a study[15] these sets were solved iteratively by neglecting, in the pure Coulomb coupling region of the integration range, the rapidly oscillating contributions to the equations. The inward-outward iteration method was used. As an application of this approach, rotational model calculations were performed for a case of multiple Coulomb-nuclear excitation of ^{238}U by 340 MeV ^{40}Ar.

In Sec. II, a concise quantum-mechanical description of inelastic scattering is given. Section III is devoted to the iterative piecewise analytical solution method. Several forms of the reference potentials and the corresponding reference solutions are described. The inward-outward iteration method, as well as the sequential method, is explained. Section IV contains the results of our investigation related to the behavior of the amplitudes and the rate of convergence of both iteration methods. In Sec. V, the excitation probabilities for ^{238}U, excited by 286 MeV ^{40}Ar and 718 MeV ^{84}Kr, are shown. Finally, as Sec. VI, conclusions are drawn and a final remark is made.

II. CONCISE DESCRIPTION OF THE SCATTERING FORMALISM

The coupled equations to be solved for the partial-wave radial functions $\psi_{Il}^{J\pi}(r)$ are

$$\left[\frac{d^2}{dr^2}+k_I^2-\frac{l(l+1)}{r^2}-\frac{2\mu}{\hbar^2}V_{\rm diag}(r)\right]\psi_{Il}^{J\pi}(r) = \frac{2\mu}{\hbar^2}\sum_{I'l'}V_{Il;I'l'}^{J\pi}(r)\psi_{I'l'}^{J\pi}(r)\ , \quad (2.1)$$

assuming a spinless projectile. Here, J, l, and I denote the total angular momentum, the orbital angular momentum, and the spin of the target nucleus, respectively. The excitation energy of the target is ϵ_I, in a state with spin I. The total angular momentum J, its projection onto the z axis, and the parity π are good quantum numbers and, therefore, Eqs. (2.1) refer to a single combination of (J,π) for the system. Let E be the center-of-mass energy in the incident channel; then, the asymptotic wave number k_I is given by

$$k_I^2=\frac{2\mu}{\hbar^2}(E-\epsilon_I)\ , \quad (2.2a)$$

and the Sommerfeld parameter η_I, which will be needed later, by

$$\eta_I=\frac{2\mu}{\hbar^2}\frac{Z_P Z_T e^2}{2k_I}\ , \tag{2.2b}$$

where μ is the reduced mass, while Z_P and Z_T represent the charge numbers of the projectile and target nucleus, respectively.

The diagonal potential is just the usual optical-model potential which is written in two parts as

$$V_{\rm diag}(r)=V^N_{\rm diag}(r)+V^C_{\rm diag}(r)\ , \tag{2.3}$$

representing the nuclear and Coulomb diagonal potentials, respectively. For the nuclear potential, the Woods-Saxon form was taken:

$$V^N_{\rm diag}(r)=-V(1+e_v)^{-1}-iW(1+e_w)^{-1}\ , \tag{2.4}$$

where

$$e_v=\exp[(r-R_v)/a_v]\ , \tag{2.5a}$$

whilst V, R_v, and a_v are the strength, the radius, and the diffuseness parameters, respectively, of the real part of the nuclear potential. Denoting the projectile and target masses by A_P and A_T, respectively, the radius R_v is given by

$$R_v=r_v(A_P^{1/3}+A_T^{1/3})\ , \tag{2.5b}$$

where r_v is the real optical radius parameter. A similar explanation applies to W and e_w concerning the imaginary part of the nuclear potential. The Coulomb potential, derived from a constant charge distribution in the target within the Coulomb radius R_c and zero outside it, has the form

$$V^C_{\rm diag}(r)=Z_P Z_T e^2\frac{1}{2R_c}\left[3-\left[\frac{r}{R_c}\right]^2\right],\quad r\le R_c \tag{2.6a}$$

$$=Z_P Z_T e^2\frac{1}{r},\quad r>R_c \tag{2.6b}$$

with

$$R_c=r_c A_T^{1/3}\ , \tag{2.6c}$$

where r_c is the Coulomb radius parameter.

Representing the coupling or transition potential by a multipole expansion of the deformed optical model and assuming rotational eigenstates for the nuclear wave functions, the elements $V^{J\pi}_{Il;I'l'}(r)$ of the coupling matrix will have the form

$$V^{J\pi}_{Il;I'l'}(r)=\sum_\lambda V^\lambda_{\rm cpl}(r)G_\lambda(Il,I'l';J)\ , \tag{2.7}$$

where the geometrical factor $G_\lambda(Il,I'l';J)$ is given by

$$G_\lambda(Il,I'l';J)=(4\pi)^{-1/2}i^{l'-l+\lambda}(-1)^{J+\lambda}\hat{I}\,\hat{I}'\hat{l}\,\hat{l}'\hat{\lambda} \times\begin{bmatrix} I' & \lambda & I\\ 0 & 0 & 0\end{bmatrix}\begin{bmatrix} l & \lambda & l'\\ 0 & 0 & 0\end{bmatrix}\begin{Bmatrix} I & l & J\\ l' & I' & \lambda\end{Bmatrix}, \tag{2.8}$$

assuming couplings within the ground-state rotational band (GSB) only. Here, the symbol $\hat{x}$ stands for $(2x+1)^{1/2}$.

The radially dependent part of the coupling potential can be described with two different terms, too:

$$V^\lambda_{\rm cpl}(r)=V^{N;\lambda}_{\rm cpl}(r)+V^{C;\lambda}_{\rm cpl}(r)\ . \tag{2.9}$$

They represent the radial dependence of the nuclear and Coulomb coupling potential, respectively. The superscript λ refers to the transferred angular momentum during the scattering process. Since only a rotational target nucleus has been considered, the nuclear coupling potential is given by a Legendre polynomial expansion with expansion coefficients for $\lambda\neq 0$:[16]

$$V^{N;\lambda}_{\rm cpl}(r)=-4\pi\int_0^1[V(1+e_v)^{-1}+iW(1+e_w)^{-1}] \times Y_{\lambda 0}(\theta)d[\cos(\theta)]\ , \tag{2.10}$$

where

$$e_v=\exp\{[r-R_v(\theta)]/a_v\}\ . \tag{2.11a}$$

The radius $R_v(\theta)$ is assumed to be given by

$$R_v(\theta)=r_v\left[A_P^{1/3}+A_T^{1/3}\left\{1+\sum_{\lambda'}\left[\beta^N_{\lambda'}Y_{\lambda' 0}(\theta)-\frac{(\beta^N_{\lambda'})^2}{4\pi}\right]\right\}\right], \tag{2.11b}$$

with the nuclear mass deformation parameters $\beta^N_{\lambda'}$.[17] The last term in the summation maintains volume to this order in the deformation parameters. A similar expression holds for e_w. The Coulomb coupling potential is expressed up to the second order in the deformation. The radial dependence has the form

$$V^{C;\lambda}_{\rm cpl}(r)=\frac{3Z_P Z_T e^2}{(2\lambda+1)R_c}\left[\beta^{C(1)}_\lambda\left[\frac{r}{R_c}\right]^\lambda+\beta^{C(2)}_\lambda(1-\lambda)\left[\frac{r}{R_c}\right]^\lambda\right],\quad r\le R_c \tag{2.12a}$$

$$=\frac{3Z_P Z_T e^2}{(2\lambda+1)R_c}\left[\beta^{C(1)}_\lambda\left[\frac{R_c}{r}\right]^{\lambda+1}+\beta^{C(2)}_\lambda(\lambda+2)\left[\frac{R_c}{r}\right]^{\lambda+1}\right],\quad r>R_c \tag{2.12b}$$

where the parameters $\beta_\lambda^{C(1)}$ and $\beta_\lambda^{C(2)}$ describe the charge deformation in the first and second orders, respectively.

To obtain solutions for $\psi_{Il}^{J\pi}(r)$, two boundary conditions have to be fulfilled. At the origin $\psi_{Il}^{J\pi}(r)$ should vanish:

$$\lim_{r\to 0}\psi_{Il}^{J\pi(I_0 l_0)}(r)=0 , \tag{2.13a}$$

whilst, for large distances, $\psi_{Il}^{J\pi}(r)$ must represent an ingoing partial wave in the entrance channel plus outgoing partial waves in all the relevant exit channels. The precise asymptotic form defines the scattering matrix elements $S_{Il;I_0l_0}^{J\pi}$:

$$\psi_{Il}^{J\pi(I_0l_0)}(r)\underset{r\to\infty}{\sim}\delta_{II_0}\delta_{ll_0}H_l^-(\eta_{I_0};k_{I_0}r)-\left[\frac{k_{I_0}}{k_I}\right]^{1/2}S_{Il;I_0l_0}^{J\pi}H_l^+(\eta_I;k_Ir) . \tag{2.13b}$$

The ingoing and outgoing Coulomb waves H_l^- and H_l^+, respectively, in terms of the well-known regular and irregular Coulomb wave functions F_l and G_l, are $H_l^\pm=(G_l\pm iF_l)$. The indices I_0,l_0 correspond to an ingoing wave in the entrance channel for $I=I_0$ and $l=l_0$.

The set of equations (2.1) has to be solved for each J value in a full range of J values. From the scattering matrix elements obtained for these J values, the cross section for the ground state and each excited state, as well as other observable quantities, can be calculated.[1]

III. ITERATIVE PIECEWISE ANALYTICAL SOLUTION METHOD

The Schrödinger equation (2.1) can be rewritten in the form

$$\left[\frac{d^2}{dr^2}+k_i^2-U_{ii}(r)\right]\psi_i(r)=\sum_{j\neq i}^{N}U_{ij}(r)\psi_j(r) ,$$
$$i=1,2,\ldots,N , \tag{3.1}$$

and the boundary condition (2.13b) as

$$\psi_i^k(r)\underset{r\to\infty}{\sim}\delta_{ik}H_i^- -\left[\frac{k_k}{k_i}\right]^{1/2}S_{ik}H_i^+ . \tag{3.2}$$

The superscript and subscript k refer to the entrance channel.

Considering some interval of the integration range with its midpoint at a radius $\bar{r}$, and introducing a reference potential $U^{\mathrm{rf}}(r)$ for that interval, Eq. (3.1) becomes

$$\left[\frac{d^2}{dr^2}+k_i^2-U_{ii}^{\mathrm{rf}}(r)\right]\psi_i(r)=\sum_{j=1}^{N}W_{ij}(r)\psi_j(r) ,$$
$$i=1,2,\ldots,N , \tag{3.3}$$

where the right-hand side contains the difference between the true potential and the reference potential.[1] Replacing the right-hand side of Eq. (3.3) by zero, several forms of the reference potential and the corresponding solutions can be considered. The form that will be used in practice depends upon the location of the integration range.

A. Constant reference potential

$$U_{ii}^{\mathrm{rf}}(r)=\bar{U}_{ii} , \tag{3.4}$$

where $\bar{U}_{ii}$ is introduced as the average value of the potential over the interval.[2,11] The reference solutions $A_i(r)$ and $B_i(r)$ are goniometric functions:

$$A_i(r)=\sin[\gamma_i(r-\bar{r})] , \tag{3.5a}$$

$$B_i(r)=\cos[\gamma_i(r-\bar{r})] , \tag{3.5b}$$

with $\gamma_i=(k_i^2-\bar{U}_{ii})^{1/2}$. If $\bar{U}_{ii}$ is real and $k_i^2<\bar{U}_{ii}$ the solutions (3.5) reduce to

$$A_i(r)=\sinh[\delta_i(r-\bar{r})] , \tag{3.6a}$$

$$B_i(r)=\cosh[\delta_i(r-\bar{r})] , \tag{3.6b}$$

in which $\delta_i=(\bar{U}_{ii}-k_i^2)^{1/2}$.

B. Linear reference potential

$$U_{ii}^{\mathrm{rf}}(r)=\bar{U}_{ii}+(r-\bar{r})\left.\frac{dU_{\mathrm{av}}(r)}{dr}\right|_{r=\bar{r}} , \tag{3.7}$$

where again $\bar{U}_{ii}$ is the average potential over that integral.[2] It should be noted that, for the first derivative, an average value for the components of the first derivative has been taken. This has to do with the analytical evaluation of integrals (3.23a) later in this paper.[1] The reference solutions are the Airy functions Ai and Bi:

$$A_i(r)=\mathrm{Ai}[\alpha(\beta_i+r)] , \tag{3.8a}$$

$$B_i(r)=\mathrm{Bi}[\alpha(\beta_i+r)] , \tag{3.8b}$$

with the constants

$$\alpha=\left[\left.\frac{dU_{\mathrm{av}}(r)}{dr}\right|_{r=\bar{r}}\right]^{1/3} \tag{3.9a}$$

and

$$\beta_i=\frac{\bar{U}_{ii}-k_i^2}{dU_{\mathrm{av}}(r)/dr\,|_{r=\bar{r}}}-\bar{r} . \tag{3.9b}$$

The Airy functions can be efficiently evaluated numerically.[2,9,10]

C. Coulomb reference potential

$$U_{ii}^{\mathrm{rf}}(r)=\frac{2\eta_i k_i}{r}+\frac{l_i(l_i+1)}{r^2} , \tag{3.10}$$

with the Sommerfeld parameter η_i and wave number k_i. The reference solutions are the regular and irregular Coulomb wave functions F_l and G_l:

$$A_i(r)=F_{l_i}(\eta_i;k_ir)\ , \tag{3.11a}$$

$$B_i(r)=G_{l_i}(\eta_i;k_ir)\ . \tag{3.11b}$$

When $\eta=0$, the reference solutions reduce to the spherical Bessel and Neumann functions which were used by Sams and Kouri.[18]

D. Integral representation of the coupled radial differential equations

If the right-hand side of Eq. (3.3) is replaced by zero, each of the resulting decoupled equations will have two linearly independent solutions:

1. the regular solution $G_i(r)$, which vanishes at the origin and is asymptotically defined as

$$G_i(r)\underset{r\to\infty}{\sim}\frac{i}{2\sqrt{k_i}}[H_i^-(\eta_i;k_ir)-S_i^0H_i^+(\eta_i;k_ir)]\ ; \tag{3.12a}$$

2. the irregular outgoing wave solution $G_i^+(r)$, which is defined by the asymptotic form

$$G_i^+(r)\underset{r\to\infty}{\sim}\frac{1}{\sqrt{k_i}}H_i^+(\eta_i;k_ir)\ . \tag{3.12b}$$

Owing to the special form of the left-hand side of Eq. (3.3), the solutions (3.12) can be expressed in terms of the linearly independent reference solutions $A_i(r)$ and $B_i(r)$ that belong to a specific form of the reference potential $U_{ii}^{\rm rf}(r)$:

$$G_i(r)=A_i(r)a_i+B_i(r)b_i \tag{3.13a}$$

and

$$G_i^+(r)=A_i(r)a_i^++B_i(r)b_i^+\ . \tag{3.13b}$$

The constant coefficients a_i,b_i and a_i^+,b_i^+ are determined by conditions of continuity at the interval boundaries.

Subsequently, the Green's function which belongs to Eq. (3.3) can be constructed; it is regular at the origin and has asymptotically an outgoing wave form:

$$G_i(r,r')=-G_i(r_<)G_i^+(r_>)\ , \tag{3.14}$$

where $r_<$ and $r_>$ are the smaller and the larger values of r and r', respectively. With an ingoing wave in the entrance channel k, the set of coupled differential equations (3.3) can be rewritten as an equivalent set of N coupled integral equations:

$$\psi_i^k(r)=G_i(r)\left[\frac{2}{i}\delta_{ik}-\int_r^\infty G_i^+(r')\sum_{j=1}^N W_{ij}(r')\psi_j^k(r')dr'\right]-G_i^+(r)\left[\int_0^r G_i(r')\sum_{j=1}^N W_{ij}(r')\psi_j^k(r')dr'\right] \tag{3.15a}$$

$$\equiv G_i(r)c_i(r)-G_i^+(r)c_i^+(r)\ . \tag{3.15b}$$

The boundary conditions are

$$c_i(\infty)=\frac{2}{i}\delta_{ik}\ , \tag{3.16a}$$

$$c_i^+(0)=0\ . \tag{3.16b}$$

In practice, however, instead of (3.16b) the approximate but numerically adequate physical boundary condition

$$c_i^+(r_0)=0 \tag{3.16c}$$

is used for a relatively small r_0, in order to prevent the set of integral equations from becoming singular.

The asymptotic value of the outgoing coefficients $c_i^+(r)$ are related to the S-matrix elements:

$$c_i^+(\infty)=S_{ik}-S_i^0\delta_{ik}\ . \tag{3.17}$$

The set of coupled integral equations (3.15) can be solved by iteration. We have concentrated our investigation on the behavior of the coefficients $c_i(r)$ and $c_i^+(r)$, instead of the wave function itself. They may be considered as the amplitudes of the functions $G_i(r)$ and $G_i^+(r)$, respectively. Two iterative methods, the inward-outward and the sequential method, have been investigated.

1. Inward-outward iteration method

In the inward-outward iteration method, the following set of coupled integral equations for the amplitudes $c_i(r)$ and $c_i^+(r)$ was considered:

$$c_i(r)=\frac{2}{i}\delta_{ik}-\int_r^\infty G_i^+(r')\sum_{j=1}^N W_{ij}(r')G_j(r')c_j(r')dr'+\int_r^\infty G_i^+(r')\sum_{j=1}^N W_{ij}(r')G_j^+(r')c_j^+(r')dr'\ , \tag{3.18a}$$

$$c_i^+(r)=\int_0^r G_i(r')\sum_{j=1}^N W_{ij}(r')G_j(r')c_j(r')dr'-\int_0^r G_i(r')\sum_{j=1}^N W_{ij}(r')G_j^+(r')c_j^+(r')dr'\ , \tag{3.18b}$$

for $i=1,2,\ldots,N$. This method was proposed by Alder, Roesel, and Morf[3] and Ichimura *et al.*[4] They used a differen-

tial form of these equations. For solving these equations iteratively, a start should be made at infinity, where the $c_j(r)$ values are known, due to the boundary condition (3.16a), although the $c_j^+(r)$ are not. However, the product $G_i^+ W_{ij} G_j^+$ oscillates rapidly over the classically allowed region of the integration range and tends to nullify the contribution of the term with $c_j^+(r)$. This will be apparent from Fig. 1. It is, therefore, justifiable to make the value of the coefficients $c_j^+(r)$ equal to zero in (3.18a) as a first estimate. Then, the first approximation of $c_i(r)$ can be generated by an inward integration of (3.18a). The values of $c_i(r)$ obtained, together with the initial condition (3.16c), can be used for an outward integration of (3.18b), where the term with $c_j(r)$ is now considered as a known inhomogeneous function. This outward integration gives a first approximation of $c_i^+(r)$ with a value at infinity, which corresponds to the first approximation of the S-matrix elements according to (3.17). The iteration procedure continues as a second inward integration of (3.18a) using the calculated values of $c_i^+(r)$ as known inhomogeneous functions and so forth, until convergence is obtained for $c_i^+(\infty)$.

For later reference, it should be noted that, in solving the set of integral equations (3.18a) for the vector $c(r)$, the coupling between its components $c_i(r)$ is retained during each step of the iteration procedure, along with the coupling implied by the "inhomogeneous" part containing the vector $c^+(r)$. The same holds *mutatis mutandis* for the components of the vector $c^+(r)$.

2. *Sequential iteration method*

Alternatively, the set of coupled integral equations for the amplitudes $c_i(r)$ and $c_i^+(r)$ can be written as

$$c_i(r)=\frac{2}{i}\delta_{ik}+\int_0^r G_i^+(r')\sum_{j=1}^N W_{ij}(r')[G_j(r')c_j(r')-G_j^+(r')c_j^+(r')]dr' - \int_0^\infty G_i^+(r')\sum_{j=1}^N W_{ij}(r')[G_j(r')c_j(r')-G_j^+(r')c_j^+(r')]dr' , \tag{3.19a}$$

$$c_i^+(r)=\int_0^r G_i(r')\sum_{j=1}^N W_{ij}(r')[G_j(r')c_j(r')-G_j^+(r')c_j^+(r')]dr' . \tag{3.19b}$$

In the sequential iteration method, which was proposed by Raynal,[5,6] the coupling potential W is considered to be a perturbation.

To illustrate the iteration procedure, the results for the nth step of the iteration for $k=1$ are written as

$$c_i^{(n)}(r)=\frac{2}{i}\delta_{i1}+\int_0^r G_i^+(r')X_i^{(n)}(r')dr' - \int_0^\infty G_i^+(r')X_i^{(n)}(r')dr' , \tag{3.20a}$$

$$c_i^{+(n)}(r)=\int_0^r G_i(r')X_i^{(n)}(r')dr' , \tag{3.20b}$$

where

$$X_i^{(n)}=W_{i1}(G_1c_1^{(n-1)}-G_1^+c_1^{+(n-1)}) + \sum_{j=2}^{i-1} W_{ij}(G_jc_j^{(n)}-G_j^+c_j^{+(n)}) + \sum_{j=i}^{N} W_{ij}(G_jc_j^{(n-1)}-G_j^+c_j^{+(n-1)}) \tag{3.21a}$$

for $i=2,3,\ldots,N$ and

$$X_i^{(n)}=W_{11}(G_1c_1^{(n-1)}-G_1^+c_1^{+(n-1)}) + \sum_{j=2}^{N} W_{1j}(G_jc_j^{(n)}-G_j^+c_j^{+(n)}) \tag{3.21b}$$

for $i=1$.

The calculation of Eqs. (3.20) starts with $i=2$, using (3.21a) under the initial conditions

$$c_j^{(0)}(r_0)=\frac{2}{i}\delta_{j1},\quad c_j^{+(0)}(r_0)=0 . \tag{3.22}$$

This component must be integrated to infinity, due to the third term in (3.20a), before the calculation can be continued for $i=3$. The iteration step ends with the integration of the first component using (3.21b).

Note also for later reference, that in solving the set of integral equations (3.19) according to an iteration procedure illustrated by (3.20), in fact, a set of coupled equations is replaced by a set of "uncoupled inhomogeneous" equations with driving terms specified by the known functions (3.21). The basic idea behind this iteration method is solving the N inhomogeneous equations (3.20) in some definite sequential order; each improved solution

$$[G_j(r)c_j^{(n)}(r)-G_j^+(r)c_j^{+(n)}(r)]$$

is immediately inserted in the inhomogeneous term of the subsequent equations, as given by the second term in (3.21a) and (3.21b). In practice, the channels have to be ordered in some special fashion with the elastic channel first, channels most strongly coupled to it next, and so on.

3. *Radial integrals*

To solve Eqs. (3.18) and (3.19), we make use of the relatively slow variation of the amplitudes $c_i(r)$ and $c_i^+(r)$ with respect to the rapid oscillations of the functions $G_i(r)$ and $G_i^+(r)$ in the classically allowed region. The r dependence of the amplitudes is weak, as long as the difference between the true potential and the reference po-

tential is small. Thus, a choice of step size has to be made so that small variations of $c_i(r)$ and $c_i^+(r)$ over an interval can be neglected.

Supposing that the true potential has been expanded in a Taylor series around $r=\bar{r}$, and assuming that, in the first iterative step, we have already integrated (3.18a), for instance, from the right up to r_r and using the value of $c_i(r_r)$, this equation yields a first-order contribution to $c_i(r_l)$ at the "left-hand" boundary r_l, provided integrals of the form

$$\int_{r_l}^{r_r} G_i(r)(r-\bar{r})^m G_j(r)dr \tag{3.23a}$$

are determined with $m=0,1,2$. Expressing $G_i(r)$, as well as $G_i^+(r)$, in the reference solutions of the constant or linear reference potentials, integrals will be obtained which can be evaluated analytically. If Airy functions are used for this purpose, then an average value for the first derivatives has to be introduced.

In the case of a Coulomb reference potential, integrals of the form

$$\int_{r_l}^{r_r} G_i(r)r^{-(\lambda+1)}G_j(r)dr \tag{3.23b}$$

are obtained for $\lambda=2,3,4,\ldots$. Expressing $G_i(r)$, as well as $G_i^+(r)$, in the regular and irregular Coulomb wave functions as the corresponding reference solutions, these integrals can be effectively evaluated by making use of recursion relations.[12]

IV. RESULTS AND DISCUSSION

In this section, we present the results related to the amplitudes $c(r)$, $c^+(r)$ and the S-matrix elements for the multiple Coulomb-nuclear excitation of ^{238}U by 718 MeV ^{84}Kr. In this case with $\eta=178.3$ and $k=39.7$ fm^{-1}, the rotational model has been considered for the target nucleus with a spin sequence according to the ground-state rotational band up to $I^\pi=24^+$ ($N=169$). The optical potential parameters were chosen as

$$\begin{aligned} &V=50.0 \text{ MeV}, \quad r_v=1.129 \text{ fm}, \quad a_v=1.10 \text{ fm}, \\ &W=32.0 \text{ MeV}, \quad r_w=1.211 \text{ fm}, \quad a_w=0.43 \text{ fm}, \\ &r_c=1.400 \text{ fm}, \end{aligned} \tag{4.1}$$

corresponding to the optical potential parameters for elastic scattering of ^{84}Kr from ^{208}Pb,[19] because the parameters for ^{238}U were not known at the time that the calculations were made.

The nuclear mass and charge deformation parameters β_λ^N and $\beta_\lambda^{C(1)}$ appearing, respectively, in (2.11b) and (2.12) are

$$\begin{aligned} &\beta_2^N=0.2370, \quad \beta_4^N=0.0, \\ &\beta_2^{C(1)}=0.2121, \quad \beta_4^{C(1)}=0.0. \end{aligned} \tag{4.2}$$

Figure 1 shows the behavior of the real parts of the amplitudes $c(r)$ and $c^+(r)$ calculated in the inward-outward method, as well as in the sequential method as a function of r for the set of quantum numbers $I_0=0$, $I=4$, $l_0=l=350$. The orbital angular momentum corresponds

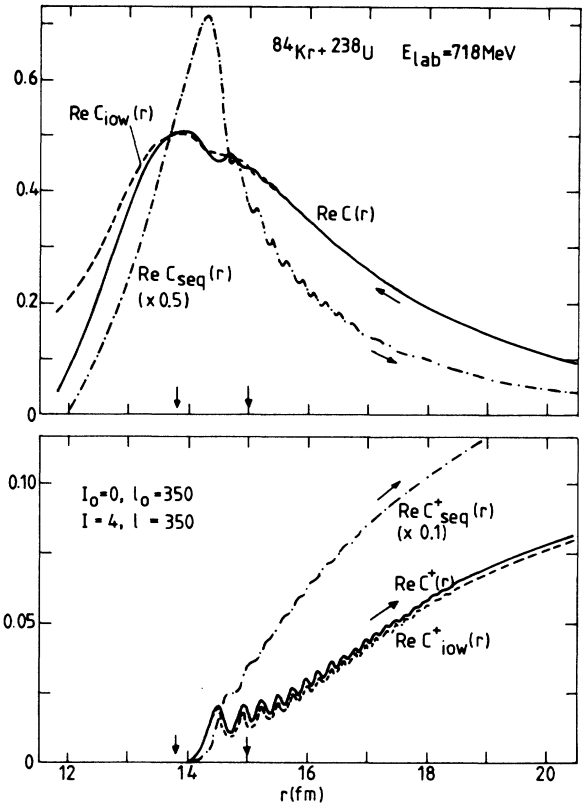

FIG. 1. This figure shows the real parts of the amplitudes $c(r)$ and $c^+(r)$ calculated in the inward-outward method, as well as in the sequential method. The dashed curves indicate the first inward-outward iteration step and the dashed-dot curves the first sequential step, whereas the full curves result from the final iteration step for both methods. The inner and outermost classical turning points are indicated by vertical arrows. This figure shows the very rapid convergence of the inward-outward iteration method when compared to the sequential one.

to a partial wave below the grazing one. The dashed curves indicate the results of the first inward-outward iteration step and the dashed-dot curves the first sequential one, whereas the full curves result from the final iteration step for both schemes. The inner and outermost classical turning points are indicated by vertical arrows. This figure shows the very rapid convergence of the inward-outward iteration scheme when compared to the sequential one. It is seen that the curves of the first inward-outward step nearly coincide with the curves of the final step. It takes only a few iteration steps to obtain convergence. However, the difference between the first and final sequential iteration steps is much larger; a lot more iteration steps are needed to obtain convergence.

We note that in the inward-outward scheme the influence of $c^+(r)$, obtained in an outward integration, on $c(r)$ during the next inward integration over the classically allowed region is rather weak. Only in the region around

the classical turning points of the decoupled set of equations is the difference between the first and final iteration steps visible in the figure. It can be seen that the amplitudes have an oscillating behavior over a limited part of the integration range outside the turning points. The step sizes must be chosen with care,[20] since they have to be such that small variations of $c(r)$ and $c^+(r)$ over an interval can be neglected. This means that the step sizes in this region, which includes the range of the optical potential for most of the orbital angular momenta, have to be made rather small. Here, the use of a constant reference potential is the most effective one; the calculations can be carried out about nine times faster when compared to the use of a linear reference potential.

The tendency of $c(r)$ and $c^+(r)$ to oscillate just outside the turning points is a general feature of these amplitudes. As a consequence, especially for light-ion scattering problems, it seems to be more effective to generate the solutions $G_i(r)$ and $G_i^+(r)$, in this part of the integration range, directly with a multistep integration method using a fixed step length.[21] The integrals appearing in (3.18) and (3.19) are then determined numerically according to commonly used methods. In this way, some calculations for the reaction ^{208}Pb(α,α')^{208}Pb(3^-, 2.6146 MeV) $E_{\rm lab}$ = 21.0 MeV have been made.

Thus, looking at the figure, the general behavior of the amplitudes may be summarized as follows: they behave monotonically inside the innermost turning point and tend to oscillate outside it before approaching constant values in the asymptotic region. This behavior determined our strategy for choosing the step sizes: they were chosen such that a constant reference potential could be used up to just a few fm outside the outermost turning point (including the optical potential), a linear reference potential for the region of strong Coulomb coupling interaction ($\approx$50 fm), and a Coulomb reference potential for the last part of the integration range (up to $\approx$1000 fm or more).

In Table I, the convergence properties of the modulus of the S-matrix elements $S^{200+}_{4,200;0,200}$ and $S^{350+}_{4,350;0,350}$ for the multiple Coulomb-nuclear excitation are shown as a function of an iteration number n for the inward-outward method, as well as for the sequential iteration method. The numbers in parentheses at the top of the columns (or alongside) denote the powers of 10 by which the underlying numbers have to be multiplied. Table II shows the same, but now the multiple excitation is caused by the Coulomb interaction only. In order to accelerate the convergence, use can be made of Padé approximants. It seems that sequences of the Padé approximants for the S-matrix elements accelerate the convergence of the original sequence when it converges, and continue to converge under many circumstances in which the original sequence diverges.[5,8] The tables also contain the results of calculations which take these approximants into account.

Table I shows that the four original sequences (without Padé acceleration) converge; the inward-outward sequences much faster than the sequential ones. This is even so when compared to the sequential sequences with Padé acceleration. It is seen that the inward-outward method requires only a few iterations to converge for the selected partial waves and does not need Padé acceleration at all.

Table II contains the iteration sequences of physically hypothetical (Coulomb excitation only) but numerically

TABLE I. Convergence properties of the modulus of two S-matrix elements for the multiple Coulomb-nuclear excitation of ^{238}U by 718 MeV ^{84}Kr are shown as a function of iteration number n for the inward-outward, as well as for the sequential iteration method. The results are presented both without and including Padé approximants.

	$\lvert S^{200+}_{4,200;0,200}\rvert$				$\lvert S^{350+}_{4,350;0,350}\rvert$			
	Inward-outward		Sequential		Inward-outward		Sequential	
n		+ Padé		+ Padé		+ Padé		+ Padé
	(−04)	(−04)	(−04)	(−04)	(00)	(00)	(00)	(00)
1	0.8809		13.604		0.2522		2.9526	
2	0.8788		48.973		0.2630		6.2808	
3	0.8788	0.8788	55.332	10.440	0.2629	0.2629	5.6258	1.2146
4			34.512	4.4840	0.2628	0.2628	3.8127	0.5459
5			13.642	1.4770	0.2628	0.2628	1.7690	0.1608
6			3.0750	0.6801			0.7991	0.2378
7			1.6980	0.8564			0.4452	0.2662
8			0.7055	0.8416			0.2320	0.2633
9			0.8625	0.8502			0.2970	0.2624
10			0.8498	0.8496			0.2446	0.2625
11			0.8492	0.8495			0.2721	0.2626
12			0.8495	0.8495			0.2582	0.2626
13			0.8495				0.2643	
14							0.2619	
15							0.2628	
16							0.2625	
17							0.2626	
18							0.2626	

TABLE II. The same as Table I, but now the multiple excitation is caused by the Coulomb interaction only.

	$\lvert S^{200+}_{4,200;0,200}\rvert$				$\lvert S^{350+}_{4,350;0,350}\rvert$			
	Inward-outward		Sequential		Inward-outward		Sequential	
n		+ Padé		+ Padé		+ Padé		+ Padé
	(00)	(00)		(01)	(00)	(00)	(00)	(00)
1	0.6028		0.24(2)		0.2376		8.1810	
2	0.0560		0.38(3)		0.2451		31.075	
3	0.2441	0.1858	0.23(4)	3.0083	0.2431	0.2430	48.045	4.9820
4	0.1980	0.1992	0.77(4)	0.4792	0.2434	0.2433	47.268	1.6410
5	0.1975	0.1987	0.19(5)	1.1744	0.2434	0.2434	34.329	0.8351
6	0.1966	0.1989	0.46(5)	1.1744			21.303	0.0600
7	0.2027	0.1992	0.13(6)	1.1744			13.342	0.3064
8	0.1980	0.1992	0.38(6)	0.8344			8.7680	0.2646
9	0.1983		0.10(7)	1.8518			6.9470	0.2181
10	0.2000		0.26(7)	1.2877			4.9176	0.2379
11	0.1990		0.67(7)	0.0608			4.0631	0.2370
12	0.1989		0.17(8)	0.1516			2.5842	0.2377
13	0.1994		0.45(8)	0.1516			2.0063	0.2377
14	0.1992		0.11(9)				1.3799	
15	0.1992		0.28(9)				0.8721	
16			0.71(9)				0.8730	
17			0.2(10)				0.2809	
18			0.5(10)				0.5803	

interesting S-matrix elements. It shows that the sequential method diverges completely. Even with the aid of Padé approximants they do not converge to the right values. Also in this case, the inward-outward method needs only a few iterations for a J value equal to 350. However, for lower J values the rate of convergence becomes less. The evaluation of the Padé approximants can accelerate the convergence in these cases. This is illustrated in the table for $J=200$. It seems that for much lower J values the inward-outward iteration method diverges too, even with the aid of Padé approximants ($J \lesssim 100$; see also Fig. 2).

In conclusion, these numerical studies show as a general feature of both iteration methods that the more important the left-hand side of Eq. (3.3) is relative to its right-hand side, the higher the rate of convergence will be. This rate is much higher for the inward-outward iteration methods compared to the sequential one, because in solving the set of coupled integral equations (3.18) for the amplitudes, the coupling between their components is still retained during the iteration procedure, as opposed to solving the set of coupled integral equations (3.19) which is replaced by a set of "uncoupled inhomogeneous" equations. The latter are solved considering the inhomogeneous terms as perturbations. The sequential iteration methods solves the equations in a certain sequential order, instead of in a straightforward way equivalent to the Born-Neumann series.

Finally, in Fig. 2, the S-matrix elements $S^{J^\pi}_{4,l=J;0,l_0=J}$ are plotted in the complex plane as a function of J. The solid curves indicate the results for the Coulomb-nuclear excitation. The S-matrix elements were calculated for the following sequence: $J=88\,216(16)$; $224\,264(8)$; $268\,296(4)$; $298\,368(2)$; $372\,400(4)$; $408\,472(8)$; $488\,552(16)$; $584\,712(32)$ and are partly given in the figure. The dashed curves indicate the results for a pure Coulomb interaction. These S-matrix elements were calculated for the following sequence: $J=88\,334(4)$; $352\,472(8)$; $488\,552(16)$; $584\,712(32)$; $776\,199\,2(64)$. The values in parentheses indicate J steps. In practice, however, it seems to be necessary to calculate the S-matrix elements only for a more limited number of appropriately spaced J values. The values of the missing S-matrix elements are obtained by interpolation. The figure shows clearly that the influence of the nuclear interaction is felt up to rather high J values (≈ 648). Since the number of target states which are coupled is reduced at high J values, the full set of coupled differential equations is calculated only up to a J value equal to about 472. For higher J values the dimension of the set can be gradually decreased.

V. COULOMB-NUCLEAR EXCITATION PROBABILITIES OF ^{40}Ar + ^{238}U AND ^{84}Kr + ^{238}U

In this section the quantum-mechanical excitation probabilities,[1] calculated in the center-of-mass system, are presented for the multiple Coulomb-nuclear excitation of ^{238}U induced by ^{40}Ar and ^{84}Kr up to high spin states of the ground-state rotational band (GSB). Also, the probabilities will be presented when pure Coulomb excitation is considered.

In Fig. 3, the probabilities for 286 MeV ^{40}Ar are plotted as a function of the scattering angle θ for the GSB states up to the one with $I^\pi=14^+$. The optical potential parameters are $V=73.0$ MeV, $W=80.3$ MeV, $r_v=r_w=1.131$ fm, $r_c=1.4$ fm, and $a_v=a_w=0.624$ fm.[22] The solid

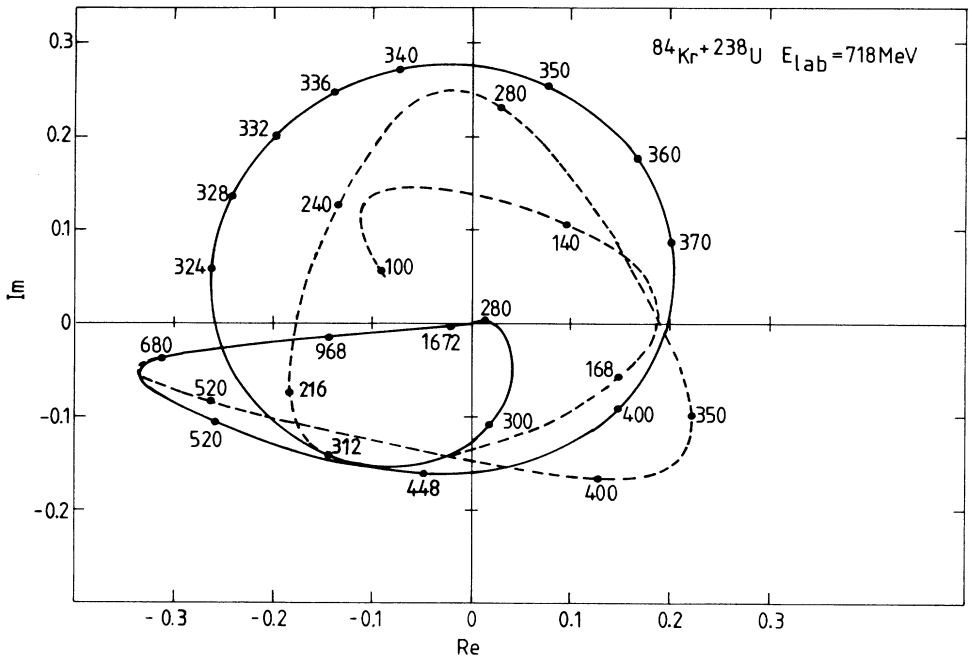

FIG. 2. The S-matrix elements $S^{J^\pi}_{4,l=J;0,l_0=J}$ are plotted in the complex plane as a function of J. The solid curves indicate the results for the Coulomb-nuclear excitation, while the dashed curves do the same for a pure Coulomb interaction. The figure shows clearly that the influence of the nuclear interaction is felt up to rather high J values.

curves show the probabilities for Coulomb-nuclear excitation ($\beta_2^N=0.237$, $\beta_4^N=0.067$, $\beta_2^{C(1)}=0.2121$, $\beta_4^{C(1)}=0.0667$). The dashed curves represent the result expected for pure Coulomb excitation. The figure shows that at scattering angles smaller than the grazing angle θ_{gr} of about 52°, the probabilities are completely determined by multiple Coulomb excitation. At this angle, the interference between the Coulomb and nuclear interactions begins to set in and corresponds to an orbital angular momentum $l_{gr}\approx 200$, given by the classical orbit relation $l=\eta\cot(\theta/2)$. Furthermore, at angles $\theta<\theta_{gr}$, which correspond to orbits much larger than l_{gr}, the angular distribution for elastic scattering deviates considerably from the typical Fresnel shape by falling below the Rutherford cross section. The quarter-point angle, i.e., the scattering angle where the summed probabilities for all final rotational states equals $\frac{1}{4}$, is about 70° and corresponds to an orbital angular momentum $l_{1/4}\approx 138$.

Similar calculations of the excitation probabilities have been performed with the same above-mentioned optical potential parameters for 340 MeV ^{40}Ar projectiles.[15] Comparing the probabilities given in this paper with ours, it seems that the extrema in the 0^+, 2^+, and 4^+ probability functions, occurring at smaller angles of course, have the same value in magnitude as our calculated values. However, the maxima of the 6^+ and 8^+ functions are about a factor of 1.8 and 4 smaller, respectively. Thus, the excitation probabilities for the high-lying members of the GSB in ^{238}U are larger for 286 MeV than for 340 MeV ^{40}Ar projectiles. This means that the interference between the Coulomb and nuclear interactions for high spin states probably can be investigated, at energies near the Coulomb barrier, most favorably.

The figure shows also the elastic scattering experimental data.[22] It is remarkable how they disagree with the elastic 0^+ curves, while on the contrary the agreement with the curve of summed probabilities is worth mentioning. Apparently, the measurements do not represent elastic data only, but also quasielastic data from the low-lying members of the GSB. A precise measurement of the elastic scattering angular distribution of 90 MeV ^{18}O on ^{184}W has given indications for this.[23]

In Figs. 4(a) and 4(b), the excitation probabilities for 718 MeV ^{84}Kr are displayed for the GSB states up to $I^\pi=16^+$. The optical potential and deformation parameters are given by (4.1) and (4.2), respectively. It is seen in these figures that for scattering angles smaller than the grazing angle of about 37° the probabilities are completely determined by multiple Coulomb excitation. Coulomb-nuclear interference starts to set in at this angle, which corresponds to $l_{gr}\approx 532$. The quarter-point angle is about 55°, corresponding to $l_{1/4}\approx 342$. Large interference effects are seen in this case.

Relating to the behavior of the probability functions in Figs. 3 and 4 at near-grazing scattering angles where the Coulomb-nuclear interference sets in, the following can be noted: *For most of the probability functions the initial Coulomb-nuclear interference is constructive (destructive) if the pure Coulomb excitation probability function for increasing scattering angles is approaching a minimum*

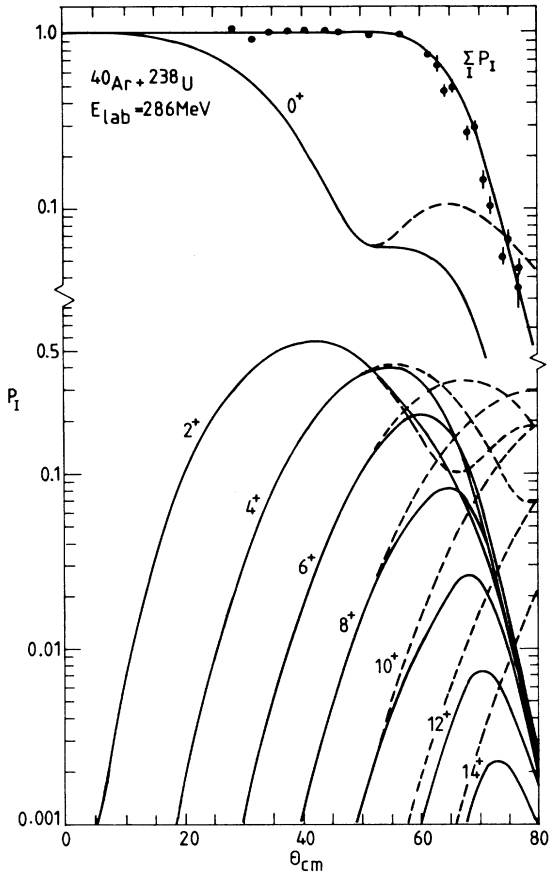

FIG. 3. The quantum-mechanical excitation probabilities P_I are plotted versus the scattering angle $\theta_{\text{c.m.}}$ for the target states up to $I^{\pi}=14^{+}$. The solid curves show the probabilities for Coulomb-nuclear excitation. The parameter set is given in the text. The dashed curves indicate the result expected for pure Coulomb excitation.

(maximum). It is remarkable that this behavior satisfies a general rule previously formulated for the behavior of the excitation probability as a function of the projectile energy near the Coulomb barrier for backward scattering from a deformed rotor[24] and based upon a semiclassical model.[17] In this model, it is assumed that the nuclear interaction can be approximated by a smooth complex potential which is largely real in the surface region.

These calculations show clearly that the excitation probabilities of excited states at scattering angles in the Coulomb-nuclear interference region can serve as sensitive probes to study peripheral processes at the deformed nuclear surface. This can be done very effectively with the method described in this paper.[25] When the S-matrix elements are calculated once for a full range of appropriately spaced J values, only those S-matrix elements with a J value corresponding to an orbital angular momentum between $l_{1/4}-\Delta l_{1/4}$ and l_{gr} have to be recalculated with a new value of the parameter set in order to fit the experimental data at scattering angles in the interference region.

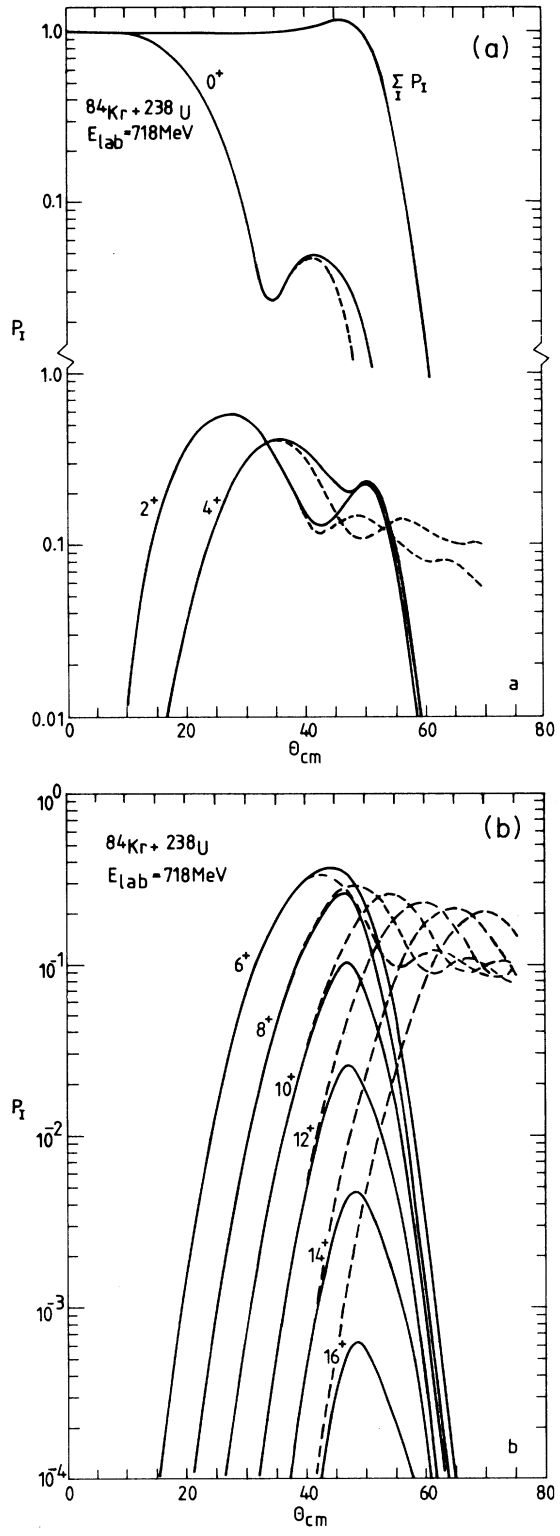

FIG. 4. (a) The quantum-mechanical excitation probabilities P_I are plotted versus the scattering angle $\theta_{\text{c.m.}}$ for the low-lying GSB target states. The solid curves show the Coulomb-nuclear probabilities. The parameter set is given in the text. The dashed curves show the result expected for pure Coulomb excitation. Large interference effects are seen. (b) The same as (a), but now for the high-lying members of the GSB.

The value of $\Delta l_{1/4}$ can be chosen relatively small. The larger the absorption in the reaction at smaller than "quarter-point" distances, the smaller this value can be taken. Thus, in practice only a restricted number of J values are needed, as can be seen in Fig. 2 for $^{84}Kr+^{238}U$.

VI. CONCLUSIONS AND FINAL REMARK

To describe quantum mechanically multiple Coulomb-nuclear excitation in heavy-ion reactions, the set of coupled differential equations of the partial-wave radial solutions is rewritten in integral form. Decomposing these solutions into two basis functions, the corresponding amplitudes of these functions satisfy a set of coupled integral equations. Expressing the basis functions in terms of appropriately chosen piecewise analytic reference solutions, the integrals appearing in this set can be evaluated analytically. The coupled set of amplitude equations is solved iteratively. The efficiency of two iteration methods, the inward-outward and the sequential one, has been investigated for test cases dealing with multiple Coulomb and nuclear excitation of ^{238}U by 286 MeV ^{40}Ar and 718 MeV ^{84}Kr up to high spin states of the ground-state rotational band. Padé approximants to the S-matrix elements were also included in both of the iteration methods. It turns out that the inward-outward iteration method converges much faster than the sequential one. In many cases, the inward-outward method does not need Padé acceleration at all, while the sequential method does. It even happens sometimes that convergent cases in the inward-outward method diverge in the sequential method aided by Padé approximants. This large difference in convergence may be explained by noting that in the inward-outward method the coupling between the amplitudes is retained during the iteration procedure, as opposed to the sequential method where the set of coupled equations is replaced by a set of "uncoupled inhomogeneous" equations. The latter are solved in a certain sequential order, treating the inhomogeneous terms as perturbations. We believe that this feature necessitates the special ordering of the channels which is not necessary in the inward-outward method.

Our numerical studies of the excitation probabilities as a function of the scattering angle for the aforementioned heavy-ion reactions show that the probability functions of the members of the ground-state rotational band satisfy a general rule at near-grazing angles, previously formulated for the excitation probability as a function of the energy near the Coulomb barrier for backward scattering from a deformed rotor.

Finally, we turn to a conclusion drawn by Rhoades-Brown *et al.*[8] in connection with the relative efficiency which they obtained for the sequential method plus Padé acceleration, compared to the method studied by us previously.[1] Based on estimates of time requirements for a case with 121 coupled equations (example 2 of Table I in Ref. 8), which calculation was not yet attempted by them, they came to the conclusion that their approach should be some 200 times faster than the conventional method, while our approach is some 30 times faster than the conventional method. Related to this conclusion, the following should be noted:

1. The conventional method they used to compare their iteration results with is based upon the Numerov multistep integration method, whereas the conventional method used in our comparison is based upon Gordon's piecewise analytic reference solutions method.[20] One integration step in this method includes many step sizes of a multistep integration method. In some circumstances, a considerable reduction of computation time (20 times for medium-weight ions and much more for heavy ions) can be obtained compared to a conventional multistep method.

2. They present estimates of time requirements for the sequential, as well as for the conventional, multistep method. However, the number of couplings per equation is taken as nine for the former, whereas for the latter 121 couplings are taken into account. This seems incorrect: it overestimates the conventional method by a factor of about 13.

Therefore, our conclusion is that the way in which Rhoades-Brown *et al.* estimate the relative efficiency (which favors their method compared to ours) is disputable. It shows that the comparison of efficiencies of methods or approaches is a delicate question without running the corresponding codes on the same computer under the same conditions such as the required accuracy. We showed from practical test cases that our approach is very efficient.[25]

ACKNOWLEDGMENTS

The author is thankful to Dr. B. J. Verhaar for critical reading of the manuscript, as well as to the computer center of Eindhoven University of Technology where the calculations were made on a Burroughs 7900 computer.

[1] L. D. Tolsma, Phys. Rev. C **20**, 592 (1979).

[2] R. G. Gordon, J. Chem. Phys. **51**, 14 (1969); R. G. Gordon, in *Methods in Computational Physics 10, Atomic and Molecular Scattering,* edited by B. Alder, S. Fernbach, and M. Rotenberg (Academic, New York, 1971), p. 81; A. Rosenthal and R.G. Gordon, J. Chem. Phys. **64**, 1621 (1976).

[3] K. Alder, F. Roesel, and R. Morf, Nucl. Phys. **A284**, 145 (1977).

[4] M. Ichimura, M. Igarashi, S. Landowne, C. H. Dasso, B. S. Nilsson, R. A. Broglia, and A. Winther, Phys. Lett. **67B**, 129 (1977).

[5] J. Raynal, in *Computing as a Language of Physics,* edited by A. Salam (IAEA, Vienna, 1972), p. 292.

[6] J. Raynal, Phys. Rev. C **23**, 2571 (1981).

[7] M. Rhoades-Brown, M. H. Macfarlane, and S. C. Pieper, Phys. Rev. C **21**, 2417 (1980).

[8] M. Rhoades-Brown, M. H. Macfarlane, and S. C. Pieper, Phys. Rev. C **21**, 2436 (1980).

[9] Z. Schulten, D. G. M. Anderson, and R. G. Gordon, J. Comput. Phys. **31**, 60 (1979); W. Moon, Comput. Phys. Commun.

22, 411 (1981).
[10]J. J. Leunissen, Eindhoven University of Technology, Department of Physics, Internal Report VDF-NK-79/07, 1979.
[11]L. Gr. Ixaru, Comput. Phys. Commun. **20**, 97 (1980); L. Gr. Ixaru, *Numerical Methods* (Reidel, Dordrecht, 1984).
[12]L. D. Tolsma, Comput. Phys. Commun. **41**, 47 (1986).
[13]L. D. Tolsma, in Proceedings of the International Conference on Nuclear Physics, Berkeley, 1980, Vol. I, p. 637.
[14]L. D. Tolsma, in Proceedings of the International Conference on Nuclear Physics, Florence, 1983, Vol. I, p. 656.
[15]A. J. Baltz, Phys. Rev. C **25**, 240 (1982).
[16]T. Tamura, Rev. Mod. Phys. **37**, 679 (1965).
[17]M. W. Guidry, H. Massmann, R. Donangelo, and J. O. Rasmussen, Nucl. Phys. **A274**, 183 (1976).
[18]W. N. Sams and D. J. Kouri, J. Chem. Phys. **51**, 4809 (1969); **51**, 4815 (1969).
[19]R. Vandenbosch, M. P. Webb, T. D. Thomas, S. W. Yates, and A. M. Friedman, Phys. Rev. C **13**, 1893 (1976).
[20]L. D. Tolsma, J. Comput. Phys. **17**, 384 (1975).
[21]N. M. Clarke, Comput. Phys. Commun. **27**, 365 (1982).
[22]J. R. Birkelund, J. R. Huizenga, H. Freiesleben, K. L. Wolf, J. P. Unik, and V. E. Viola, Jr., Phys. Rev. C **13**, 133 (1976).
[23]C. E. Thorn, M. L. LeVine, J. J. Kolata, C. Flaum, R. D. Bond, and J. C. Sens, Phys. Rev. Lett. **38**, 384 (1977).
[24]M. W. Guidry, P. A. Butler, R. Donangelo, E. Grosse, Y. El Masri, I. Y. Lee, F. S. Stephens, R. M. Diamond, L. L. Riedinger, C. R. Bingham, A. C. Kahler, J. A. Vrba, E. L. Robinson, and N. R. Johnson, Phys. Rev. Lett. **40**, 1016 (1978).
[25]L. D. Tolsma, Comput. Phys. Commun. **37**, 245 (1985); L. D. Tolsma, in *Supercomputer Applications,* edited by A. H. L. Emmen (North-Holland, Amsterdam, 1985), p. 227.